



1 **Impact of Biomass Burning emission on total peroxy nitrates: fire**  
2 **plume identification during the BORTAS campaign**

3

4 **Eleonora Aruffo<sup>1,2</sup>, Fabio Biancofiore<sup>1,2</sup>, Piero Di Carlo<sup>1,2</sup>, Marcella Busilacchio<sup>1</sup>, Marco Verdecchia<sup>1,2</sup>,**  
5 **Barbara Tomassetti<sup>1,2</sup>, Cesare Dari-Salisburgo<sup>1</sup>, Franco Giammaria<sup>1</sup>, Stephane Bauguitte<sup>3</sup>, James Lee<sup>4</sup>,**  
6 **Sarah Moller<sup>4</sup>, James Hopkins<sup>4</sup>, Shalini Punjabi<sup>4</sup>, Stephen Andrews<sup>4</sup>, Alistair C. Lewis<sup>4</sup>, Paul I. Palmer<sup>5</sup>,**  
7 **Edward Hyer<sup>6</sup>, Michael Le Breton<sup>7</sup>, Carl Percival<sup>7</sup>**

8

9 [1] Center of Excellence CETEMPS, Universita' dell'Aquila, Via Vetoio, Coppito, L'Aquila, Italy,  
10 [2] Department of Physical and Chemical Sciences, University of L'Aquila, Coppito L'Aquila, Italy,  
11 [3] Facility for Airborne Atmospheric Measurements, Bedfordshire, UK,  
12 [4] Department of Chemistry, University of York, York, UK,  
13 [5] School of GeoSciences, University of Edinburgh, UK.  
14 [6] Marine Meteorology Division, Naval Research Laboratory, Monterey, California, USA.  
15 [7] The Centre for Atmospheric Science, School of Earth, Atmospheric and Environmental Science,  
16 University of Manchester, UK.

17

18 Correspondence to: E. Aruffo (eleonora.aruffo@aquila.infn.it)

19

20 **Abstract**

21 The total peroxy nitrates ( $\Sigma$ PNs) concentrations have been measured using a thermal dissociation  
22 laser induced fluorescence (TD-LIF) instrument during the BORTAS campaign, which focused on  
23 the impact of boreal biomass burning emissions on air quality in the Northern hemisphere. The strong  
24 correlation observed between the  $\Sigma$ PNs concentrations and those of the carbon monoxide (CO), a  
25 well-known pyrogenic tracer, suggests the possible use of the  $\Sigma$ PNs concentrations as marker of the  
26 biomass burning (BB) plumes. We applied both statistical and percentile methods to the  $\Sigma$ PNs  
27 concentrations, comparing the percentage of BB plume selected using these methods with the  
28 percentage evaluated applying the approaches usually used in literature. Moreover, adding the  
29 pressure threshold ( $\sim 750$  hPa) to  $\Sigma$ PNs, HCN and CO, as ancillary parameter, the BB plume  
30 identification is improved. An artificial recurrent neural network (ANN) model was adapted to  
31 simulate the concentrations of  $\Sigma$ PNs and the HCN including as input parameters  $\Sigma$ PNs, HCN, CO  
32 and atmospheric pressure, to verify the specific role of these input data to better identify BB plumes.

33



## 1 **1. Introduction**

2 Biomass burning (BB) events are an important source of many trace gases and particles in the  
3 atmosphere [Crutzen et al., 1979; Crutzen and Andreae, 1990; Goode et al., 2000; Andreae and  
4 Merlet, 2001,]. The signature of BB emission in a plume detected far away from the fire is usually  
5 the increase of the atmospheric concentration of pyrogenic species including carbon dioxide (CO<sub>2</sub>),  
6 carbon monoxide (CO), methane (CH<sub>4</sub>) and a series of volatile organic compounds (VOCs),  
7 accompanied by elevated concentrations of peroxyacyl nitrate (PAN) [e.g., Goode et al., 2000; Cofer  
8 et al., 1998; Bertschi et al., 2004; Dibb et al., 2003; Lewis et al., 2007, Tereszchuk et al 2011].

9 In recent years, several studies have focused on boreal forest fires to quantify the influence of boreal  
10 fire emissions on the Earth-Atmosphere system and subsequent impact on the climate. Boreal forest  
11 fires (<http://www.borealforest.org>) affect mainly Siberia, Canada and Alaska and occur generally  
12 from May to October (Lavoué et al., 2000). In the past three decades occurrence of boreal forest fires  
13 and areas burned over Canada have both increased (Gillett et al., 2004; Rinsland et al., 2007; Marlon  
14 et al., 2008). The impact of boreal BB on atmospheric chemistry is triggered by the large emissions  
15 of CO, NO<sub>x</sub> (NO + NO<sub>2</sub>), nonmethane hydrocarbons (NMHC) and other NO<sub>y</sub> species (Alvarado et  
16 al., 2010; Parrington et al., 2012): NO<sub>y</sub> = NO<sub>x</sub> + ∑RONO<sub>2</sub> + ∑RO<sub>2</sub>NO<sub>2</sub> + HNO<sub>3</sub> + HONO + 2N<sub>2</sub>O<sub>5</sub>  
17 + NO<sub>3</sub>, where RONO<sub>2</sub> are total alkyl nitrates (known also as ∑ANs), RO<sub>2</sub>NO<sub>2</sub> are total peroxy nitrates  
18 (known also as ∑PNs), HNO<sub>3</sub> is nitric acid, HONO is nitrous acid, N<sub>2</sub>O<sub>5</sub> is dinitrogen pentoxide and  
19 NO<sub>3</sub> is nitrate radical. These species can influence the formation of O<sub>3</sub> in the Arctic and at the mid  
20 latitudes: the role of boreal BB emissions on the O<sub>3</sub> concentration has been studied by several authors  
21 showing situations where O<sub>3</sub> concentrations increased and others where it was unaffected (e.g. Wofsy  
22 et al., 1992; Jacob et al., 1992; Mauzerall et al., 1996; Wotawa and Trainer, 2000; Val Martin et al.,  
23 2006; Real et al., 2007; Leung et al., 2007, Jaffe and Wigder, 2012; Parrington et al., 2012). The  
24 formation of NO<sub>x</sub> oxidation products (∑ANs, ∑PNs and HNO<sub>3</sub>) plays a very important role in  
25 controlling the ozone budget as they inhibit local O<sub>3</sub> formation (Leung et al., 2007). Many  
26 investigations demonstrated the central role played by the peroxy acetyl nitrate (PAN), one of the  
27 most common PNs, in BB plume chemistry and, specifically, in the NO<sub>x</sub> oxidation processes (Jacob  
28 et al., 1992; Hudman et al., 2007). Alvarado et al. (2010) demonstrated the rapid PAN formation  
29 occurring within 1-2 hours after the emissions by a BB plume: the 40% of the NO<sub>x</sub> initially emitted  
30 by the fires is rapidly converted into PAN and the 20% into NO<sub>3</sub> (particles phase). In aged plumes,  
31 PAN can represent up to the 67% of the NO<sub>y</sub> budget (Alvarado et al., 2010).

32 Analysis of chemistry of BB emissions starts with identifying a BB plume; however, previous studies  
33 have used multiple different approaches for the identification and classification of BB plumes. Many  
34 studies have recognized CO as a pyrogenic species (Crutzen et al., 1979; Andreae and Merlet, 2001;

2



1 Lewis et al., 2013), but other chemical species, such as HCN and CH<sub>3</sub>CN, have also been employed  
2 to identify a BB plume. In the assembly of the BORTAS data analysis, different procedures have  
3 been applied. Palmer et al. (2013) identified a threshold for each of these species that would separate  
4 air masses produced during boreal BB from background air masses; they defined a BB plume when  
5 the CO, hydrogen cyanide (HCN) and acetonitrile (CH<sub>3</sub>CN) levels are higher than 148 ppb, 122 ppt  
6 and 150 ppt, respectively. These thresholds correspond to the 99<sup>th</sup> percentile ( $\sim$ mean $\pm$ 3 $\sigma$ ) of the data  
7 for the species measured during the flight B625, in which there was not a significant correlation  
8 between the CO and the CH<sub>3</sub>CN. In the context of the BORTAS campaign, Lewis et al. (2013)  
9 classified the air masses in three groups: 1) background if CO < 200 ppb; 2) BB plumes if the CO >  
10 200 ppb with the presence of pyrogenic species such as furan or furfural; 3) anthropogenic plumes if  
11 CO > 200 ppb with the absence of furan or furfural. Le Breton et al (2013) observed a strong  
12 correlation between the HCN, CO and CH<sub>3</sub>CN indicating the utilisation of HCN as a BB marker.  
13 They identified a BB plume using a standard deviation ( $\sigma$ ) method applied to the 1 Hz HCN  
14 measurements: when the HCN concentrations were 6 $\sigma$  above the background for the flights in  
15 analysis, they flagged the air mass as a BB plume. The 6 $\sigma$  threshold was chosen since it produces the  
16 highest R<sup>2</sup> values for the correlation between the HCN and the CO. For other experiments different  
17 methods for the BB plumes identification have been suggested: 1) Holzinger et al. (2005) used a  
18 method similar to that used by Le Breton et al. (2013); their results highlighted a good correlation  
19 between acetonitrile (CH<sub>3</sub>CN) and CO and they identified BB plumes by significant peaks in the  
20 CH<sub>3</sub>CN volume mixing ratio (using a threshold of 3 $\sigma$  above the background level); 2) Vay et al.  
21 (2011) identified a plume when CO > 160 ppb (the median observed CO concentration at the surface),  
22 CH<sub>3</sub>CN > 225 ppt (threshold characterized by an evident enhancement in CH<sub>3</sub>CN mixing ratios) or  
23 HCN > 500 ppt (when the CH<sub>3</sub>CN was not available); 3) Hornbrook et al. (2011) defined a plume by  
24 elevated fire tracers above the local background using thresholds of CH<sub>3</sub>CN > 200 ppt, HCN > 400  
25 ppt and CO > 175 ppb; 4) Tereszchuk et al. (2011) selected as BB plumes air masses when HCN >  
26 350 ppt, assuming that background concentrations of HCN in the free troposphere range between 225  
27 ppt and 250 ppt and, finally, 5) Alvarado et al. (2010) observed the enhancement of CO correlated  
28 with an enhancement in HCN and CH<sub>3</sub>CN; they identified a plume as having a CO concentration at  
29 least 20 ppb above the background level.

30 An aircraft campaign was conducted in Nova Scotia (Canada) with the principle purpose of evaluating  
31 the BB emissions impact on tropospheric photochemistry in the Northern Hemisphere. This work is  
32 part of the BORTAS project (quantifying the impact of BOREal forest fires on Tropospheric oxidants  
33 over the Atlantic using Aircraft and Satellites). This project included a field campaign using a  
34 research aircraft (the FAAM BAe-146) conducted in July and August 2011 during the boreal forest



1 fire season in Canada. Further details about this project can be found in Palmer et al. (2013) and at  
2 <http://www.geos.ed.ac.uk/research/eochem/bortas/>.  
3 In our analysis of the BORTAS aircraft measurement data, we found a good correlation between the  
4  $\Sigma$ PNs and CO, suggesting the potential of  $\Sigma$ PNs as pyrogenic tracer to discriminate the BB plumes.  
5 Therefore, in this work we propose two different methods to use the  $\Sigma$ PNs as BB tracer: a statistical  
6 approach using the  $6\sigma$  threshold and the 99<sup>th</sup> percentile of the  $\Sigma$ PNs calculated for the B625 flight.  
7 We evaluated all of the methods described above to our dataset to compare the results of different  
8 methods to identify BB plumes. We show also that, in some cases, the introduction of meteorological  
9 parameters, which take into account of the air masses vertical position in the atmosphere,  
10 discriminates better the origin of the air masses and, then, helps to select more precisely a BB plume.  
11 Finally, in order to refine the method we adapted an artificial neural network model and we used it to  
12 simulate the  $\Sigma$ PNs and the HCN in two different procedures to BB plume identification: 1) using as  
13 inputs the CO, NO, CH<sub>3</sub>CN; 2) adding to the inputs also the pressure.

14

## 15 **2. Experimental**

### 16 **2.1 TD-LIF measurements: NO<sub>2</sub>, $\Sigma$ PNs, $\Sigma$ ANs**

17 A detailed description of the BORTAS experiment can be found in Palmer et al. (2013), along with  
18 a description of the FAAM BAe-146 instrumental payload. During BORTAS campaign (Canada,  
19 summer 2011), observations of NO<sub>2</sub>, total  $\Sigma$ PNs,  $\Sigma$ ANs, on board the British FAAM BAe 146  
20 research aircraft, were carried out using the TD-LIF (Thermal Dissociation – Laser Induced  
21 Fluorescence) instrument developed at the University of L'Aquila (Italy) (Dari-Salisburgo et al.,  
22 2009; Di Carlo et al., 2013). Briefly, this technique uses direct measurements of NO<sub>2</sub> molecules by  
23 Laser Induced Fluorescence (LIF), whereas  $\Sigma$ PNs,  $\Sigma$ ANs and HNO<sub>3</sub> are thermally dissociated into  
24 NO<sub>2</sub> heating the air sample at 200°C, 400 °C and 550°C, respectively (Day et al., 2002; Di Carlo et  
25 al., 2013).

26

### 27 **2.2 Ancillary measurements: O<sub>3</sub>, CO, VOCs**

28 Table 1 reports a number of the compounds measured on-board the BAe-146 aircraft during the  
29 BORTAS campaign, specifically those used in this analysis. The instrument used to measure O<sub>3</sub> was  
30 a commercial UV absorption system Model 49C (Thermo Environmental Corp.) (Wilson and Birks,  
31 2006). CO was measured using the vacuum ultraviolet (VUV) resonance fluorescence technique. This  
32 type of CO instrument was applied to aircraft measurement by Gerbig et al. (1999). NO was measured  
33 using a single-channel chemiluminescence instrument manufactured by Air Quality Design, Inc.



1 (Colorado, USA, <http://www.airqualitydesign.com/>) (Lee et al. 2009; Reidmiller et al. 2010).  
2 Concentrations of volatile organic compounds (VOCs) ranging from C5 to C12 were measured by an  
3 automatic gas chromatograph system equipped with a mass spectrometer GC-MS (Purvis et al. 2013).  
4 C2-C7 hydrocarbons and C2-C5 oxygenated volatile organic compounds (o-VOCs) including  
5 alcohols, aldehydes, ketones and ethers were obtained by the University of York (UK) using whole  
6 air sampling (WAS) coupled to an automatic gas chromatograph system equipped with a mass  
7 spectrometer and a flame ionization detector (GC-MS/FID) (Hopkins et al. 2003). Measurements of  
8 a suite of volatile organic compounds: CH<sub>3</sub>CN, C<sub>3</sub>H<sub>6</sub>O, C<sub>5</sub>H<sub>8</sub>, MVK+MACR, C<sub>4</sub>H<sub>8</sub>O, C<sub>6</sub>H<sub>6</sub>, C<sub>7</sub>H<sub>8</sub>,  
9 C<sub>10</sub>H<sub>16</sub> were made by proton transfer reaction mass spectrometry (PTR MS) (Murphy et al. 2010).  
10 Finally, a chemical ionisation mass spectrometer (CIMS) was used for measuring hydrogen cyanide  
11 (HCN) from biomass burning events (Le Breton et al., 2013).

12

13 **Table 1.** List of FAAM BAe-146 instrumental payload and observed compounds used in the analysis  
14 in this paper. A description of the FAAM BAe-146 instrumental payload, with accuracy and detection  
15 limit, is reported in Palmer et al. (2013).

Species	Method	Reference
CO	VUV resonance/fluorescence	Gerbig et al. (1999)
O <sub>3</sub>	UV absorption	Wilson and Birks (2006)
NO <sub>2</sub> , ΣRO <sub>2</sub> NO <sub>2</sub> , ΣRONO <sub>2</sub> , NO <sub>y</sub>	TD-LIF	Dari-Salisburgo et al. (2009); Di Carlo et al. (2013)
NO	AQD chemiluminescence	Lee et al. 2009; Reidmiller et al. 2010
C <sub>5</sub> –C <sub>12</sub> VOCs	GC-MS	Purvis et al. (2013)
C <sub>2</sub> –C <sub>7</sub> NMHCs, acetone CH <sub>3</sub> OH	WAS-GC	Hopkins et al. (2003)
HCN	CIMS	Le Breton et al. (2013)



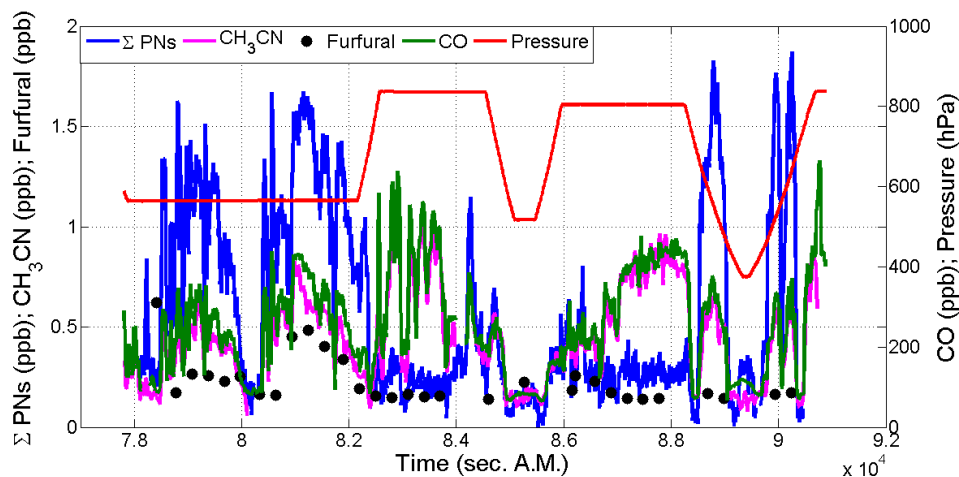
CH <sub>3</sub> CN, C <sub>3</sub> H <sub>6</sub> O, C <sub>5</sub> H <sub>8</sub> , MVK+MACR, C <sub>4</sub> H <sub>8</sub> O, C <sub>6</sub> H <sub>6</sub> , C <sub>7</sub> H <sub>8</sub> , C <sub>10</sub> H <sub>16</sub>	PTR-MS	Murphy et al. (2010)
---------------------------------------------------------------------------------------------------------------------------------------------------------------------------------------------------------------------------------------	--------	----------------------

1

### 2 3. Plume identification

3 Figure 1 shows the time series of the species investigated in this paper ( $\Sigma$ PNs, acetonitrile, HCN, CO  
 4 and furfural) for one of the flights analysed (B623), illustrated as an example. The  $\Sigma$ PNs trends shows  
 5 exactly the same structures present on CO and CH<sub>3</sub>CN, with the exception of two plumes (in the  
 6 temporal intervals of  $(8.2 - 8.4) \times 10^4$  and  $(8.6 - 8.8) \times 10^4$  seconds After Midnight (A.M.)) that are  
 7 extensively analysed in the next sections. Moreover, the furfural shows similar trend for the first part  
 8 of the flight; since CO, acetonitrile, HCN and Furfural are a known BB tracers (Lewis et al. 2013;  
 9 Palmer et al. 2013; Le Breton et al., 2013), the significant correlation between the  $\Sigma$ PNs and those  
 10 species suggests that the  $\Sigma$ PNs also originated at the same boreal biomass burning source and that it  
 11 can be used as additional chemical species for the identification of the BB plumes.

12



13

14 **Figure 1.** Time series of  $\Sigma$ PNs, CH<sub>3</sub>CN, Furfural, CO and pressure during the flight B623, shown as  
 15 example.

16



1 As described in the introduction, recently different compounds (CO, HCN or CH<sub>3</sub>CN) and different  
2 concentrations thresholds have been introduced as tracers to establish if the air mass monitored is  
3 affected by forest fire emissions or not. These methods are summarized in Table 2.

4 **Table 2.** Methods to identify BB plumes.

	Methods
Holzinger et al. (2005)	CH <sub>3</sub> CN > 3σ
Alvarado et al. (2010)	CO increase of at least 20 ppb respect to the background and its correlation with HCN or CH <sub>3</sub> CN
Vay et al. (2011)	CO > 160 ppb, HCN > 500 ppt or CH <sub>3</sub> CN > 225 ppt
Hornbrook et al. (2011)	CO > 175 ppb, HCN > 400 ppt, CH <sub>3</sub> CN > 200 ppt
Tereshchuk et al. (2011)	HCN > 350 ppt
Lewis et al. (2013)	CO > 200 ppb and presence of furan or furfural
Palmer et al. (2013)	CO > 148 ppb, HCN > 122 ppt and CH <sub>3</sub> CN > 150 ppt
Le Breton et al. (2013)	HCN > 6σ
This work	∑PNs > 6σ or ∑PNs > 418 ppt

5

6 In our analysis we tested the use of the concentration profiles of ∑PNs as possible identifier of BB  
7 plumes. We applied two different methods: 1) evaluating the 99<sup>th</sup> percentile of the ∑PNs  
8 concentrations measured during the background flight B625 (as done by Palmer et al., 2013) and  
9 using this value as threshold to distinguish air masses emitted by fires; 2) applying the statistical  
10 approach (σ method). In the first case, we calculate the 99<sup>th</sup> percentile of the 1 second ∑PNs data  
11 sampled during the B625 finding a threshold of 418 ppt. In the second case, first we selected the parts  
12 of each flight identifiable as background and, then, we evaluated for these data the mean and the  
13 standard deviation of the ∑PNs; after that, we identified as BB plumes the parts of each flight in  
14 which the difference between ∑PNs concentrations and the background level were higher than 6  
15 standard deviations of the background. This threshold has been evaluated calculating the correlation  
16 coefficients between the ∑PNs and the CO varying the sigma threshold between 10σ and 3σ for each  
17 flight in which the ∑PNs showed evident and clear plumes (such as B622 and B623): we found that  
18 the maximum R occurred when we selected the BB plume using the 6σ threshold. In Table 3 are  
19 summarized the correlation coefficients R and the percentage of flight selected as BB plume obtained  
20 for all the flights in analysis using both the methods just described. Moreover, we indicated the  
21 percentage of flight identified as BB plume applying all the methods listed in Table 2 to our dataset.



1

2 **Table 3.** Correlation coefficient (R) and percentage (%) of each flight of the BORTAS campaign  
 3 selected as BB plume using both the  $\Sigma$ PNs methods ( $6\sigma$  and 99<sup>th</sup> percentile thresholds) and percentage  
 4 (%) of BB plume evaluated for each BORTAS flight using the methods applied in other studies.

Flight	This study ( $\Sigma$ PNs methods)				Other studies		
	$6\sigma$		$\Sigma$ PNs > 0.418 99 <sup>th</sup> percentile			%	Comments
	R	%	R	%			
<b>B619a</b>	-	0	-0.045	13.5	Palmer et al.	0	Only CO
					Vay et al.	0	Only CO
					Hornbrook et al.	0	Only CO
					Holzinger et al.	-	No CH <sub>3</sub> CN
					Alvarado et al.	1.3	Only CO
					Lewis et al.	0	No Furfural – CO < 200
					Tereszczuk et al.	-	No HCN
					Le Breton et al.	-	No HCN
<b>B619b</b>	-	0	-0.168	1.3	Palmer et al.	0	Only CO
					Vay et al.	0	Only CO
					Hornbrook et al.	0	Only CO
					Holzinger et al.	-	No CH <sub>3</sub> CN
					Alvarado et al.	0	Only CO
					Lewis et al.	0	No Furfural – CO < 200
					Tereszczuk et al.	-	No HCN
					Le Breton et al.	-	No HCN
<b>B620</b>	-	0	-	0	Palmer et al.	0	Only CO
					Vay et al.	0	Only CO
					Hornbrook et al.	0	Only CO
					Holzinger et al.	-	No CH <sub>3</sub> CN
					Alvarado et al.	5.1	Only CO
					Lewis et al.	0	No Furfural - CO < 200
					Tereszczuk et al.	-	No HCN
					Le Breton et al.	-	No HCN

8



<b>B621a</b>	0.953	59.1	0.951	77.6	Palmer et al.	58.9	
					Vay et al.	23.1	
					Hornbrook et al.	32.5	
					Holzinger et al.	72.3	
					Alvarado et al.	76.8	
					Lewis et al.	-	No Furfural – CO > 200
					Tereszczuk et al.	41.6	
					Le Breton et al.	47.7	
<b>B621b</b>	0.644	3.6	0.644	3.6	Palmer et al.	2.0	NO CH <sub>3</sub> CN in the plume; missing data of HCN in the flight (only a plume)
					Vay et al.	0	NO CH <sub>3</sub> CN in the plume; missing data of HCN in the flight (only a plume)
					Hornbrook et al.	0	NO CH <sub>3</sub> CN in the plume; missing data of HCN in the flight (only a plume)
					Holzinger et al.	0.6	Missing data for the CH <sub>3</sub> CN in the flight
					Alvarado et al.	14.4	
					Lewis et al.	-	No Furfural – CO > 200
					Tereszczuk et al.	26.3	
					Le Breton et al.	32.4	Missing data (only a plume)
<b>B622</b>	0.867	51.9	0.864	55.8	Palmer et al.	52.2	
					Vay et al.	7.2	
					Hornbrook et al.	10.7	
					Holzinger et al.	50.0	
					Alvarado et al.	74.2	
					Lewis et al.	45.6	



					Tereszchuk et al.	10.4	
					Le Breton et al.	51.1	
<b>B623</b>	0.804	41.2	0.776	42.6	Palmer et al.	76.9	No HCN
					Vay et al.	73.6	No HCN
					Hornbrook et al.	70.5	No HCN
					Holzinger et al.	80.5	
					Alvarado et al.	85.6	
					Lewis et al.	71.0	
					Tereszchuk et al.	-	No HCN
					Le Breton et al.	-	No HCN
<b>B626a</b>	-	0	-	0	Palmer et al.	0	No HCN
					Vay et al.	0	No HCN
					Hornbrook et al.	0	No HCN
					Holzinger et al.	0.6	
					Alvarado et al.	2.0	
					Lewis et al.	0	No Furfural – CO < 200
					Tereszchuk et al.	-	No HCN
					Le Breton et al.	-	No HCN
<b>B626b</b>	0.755	8.1	0.259	0.4	Palmer et al.	8.6	No CH <sub>3</sub> CN
					Vay et al.	5.6	No CH <sub>3</sub> CN
					Hornbrook et al.	3.7	No CH <sub>3</sub> CN
					Holzinger et al.	-	No CH <sub>3</sub> CN
					Alvarado et al.	8.5	
					Lewis et al.	1.9	
					Tereszchuk et al.	15.1	
					Le Breton et al.	19.3	
<b>B627</b>	-	0	0.073	11.0	Palmer et al.	0	No HCN
					Vay et al.	0	No HCN
					Hornbrook et al.	0	No HCN
					Holzinger et al.	0.3	
					Alvarado et al.	3.1	
					Lewis et al.	0	No Furfural – CO < 200
					Tereszchuk et al.	-	No HCN



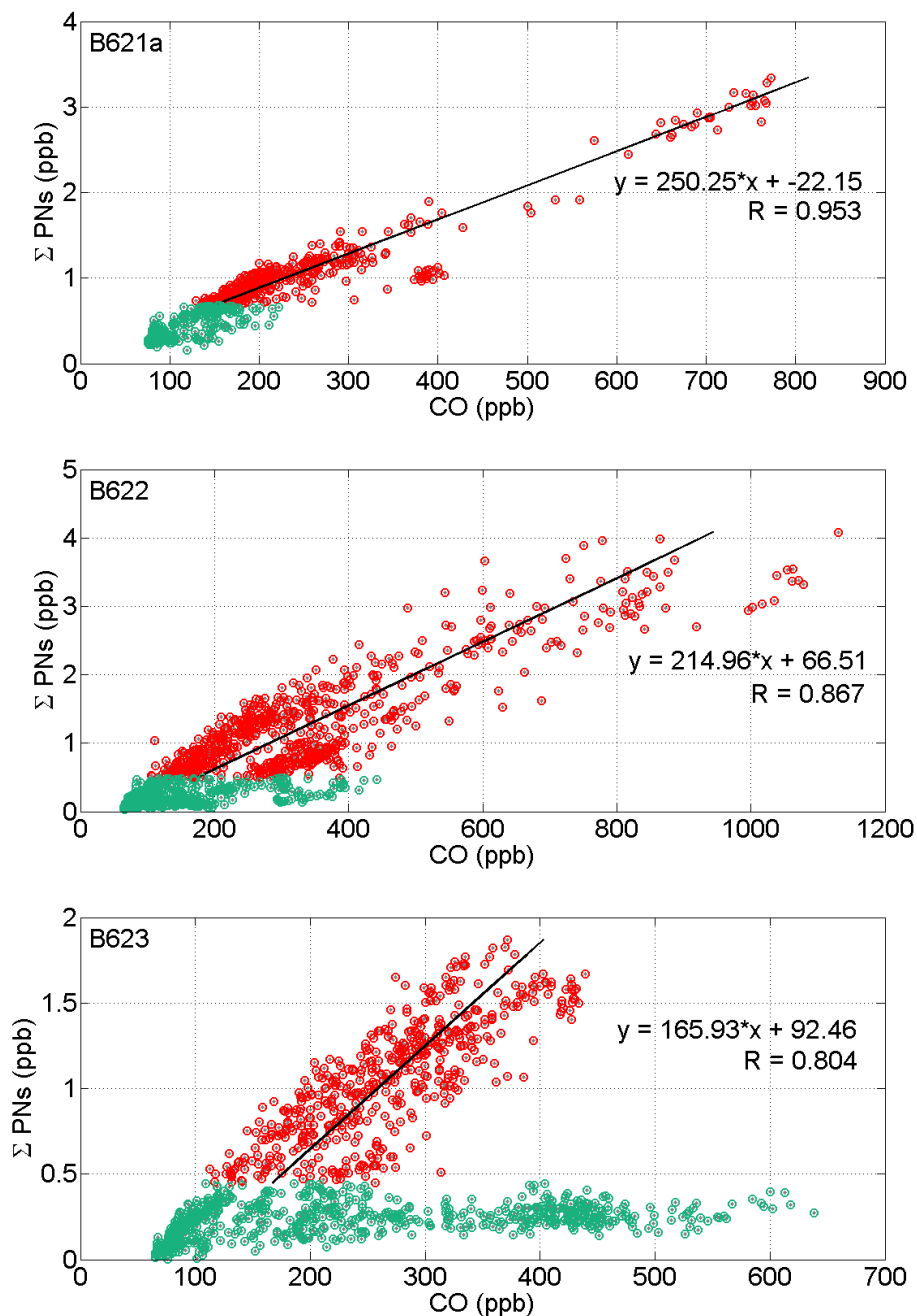
					Le Breton et al.	-	No HCN
<b>B628a</b>	-	0	-	0	Palmer et al.	0	
					Vay et al.	0	
					Hornbrook et al.	0	
					Holzinger et al.	0.3	
					Alvarado et al.	21.0	
					Lewis et al.	0	No Furfural – CO < 200
					Tereshchuk et al.	0	
					Le Breton et al.	40.1	
<b>B628b</b>	0.477	11.9	0.540	10.6	Palmer et al.	2.5	No HCN
					Vay et al.	0	No HCN
					Hornbrook et al.	0	No HCN
					Holzinger et al.	6.3	
					Alvarado et al.	61.1	
					Lewis et al.	0	No Furfural – CO < 200
					Tereshchuk et al.	-	No HCN
					Le Breton et al.	-	No HCN
<b>B629</b>	-0.036	6.4	-0.010	5.7	Palmer et al.	3.9	No HCN
					Vay et al.	1.1	No HCN
					Hornbrook et al.	0	No HCN
					Holzinger et al.	7.6	
					Alvarado et al.	6.2	
					Lewis et al.	0	No Furfural – CO < 200
					Tereshchuk et al.	-	No HCN
					Le Breton et al.	-	No HCN
<b>B630</b>	0.007	2.0	0.005	2.6	Palmer et al.	12.0	No HCN
					Vay et al.	5.1	No HCN
					Hornbrook et al.	2.4	No HCN
					Holzinger et al.	26.2	
					Alvarado et al.	42.9	
					Lewis et al.	-	No Furfural – peak with CO > 200
					Tereshchuk et al.	-	No HCN



					Le Breton et al.	-	No HCN
--	--	--	--	--	------------------	---	--------

1

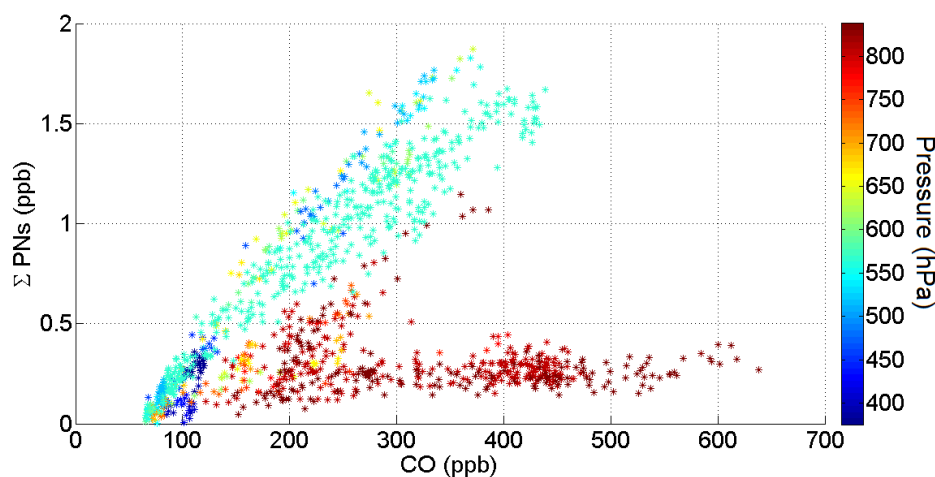
2 In order to make the analysis as accurate as possible, the double flights were separated and applied  
 3 all the methods in each part of the flights taking into account of different Canadian regions and  
 4 different hours of the day during which we were flying. The  $\Sigma$ PNs methods give, in most cases,  
 5 results in agreement with each of the methods that use CO, HCN and CH<sub>3</sub>CN (see table 3) and allow  
 6 to discriminate 3 flights (B621a, B622 and B623) in which a significant percentage (higher than the  
 7 40% with R ranging between 0.804 and 0.953) of the data have been collected sampling air masses  
 8 emitted by biomass burning. Moreover, these results are also in agreement with what is found  
 9 applying the approaches suggested in other studies. We found three flights (B621b, B626b and  
 10 B628b) in which the majority of the methods show that a small percentage (less than 10% with R  
 11 ranging between 0.477 and 0.755) of data can be identified as BB plumes (see table 3). In six flights  
 12 (B619a, B619b, B620, B626a, B627 and B628a) the  $\Sigma$ PNs  $6\sigma$  method suggests, in agreement with  
 13 the majority of the other techniques, a dominance of background air masses sampled; the 99<sup>th</sup>  
 14 percentile method applied to the  $\Sigma$ PNs for the flights B619a, B619b and B627 show a small fraction  
 15 of flight selected as BB. Moreover, the R values between the  $\Sigma$ PNs and the CO in those points is so  
 16 low (or even negative) to suggest that these parts of the flights are not ascribable as BB plume. The  
 17 flights B629 and B630 present a small percentage of the flight identified as BB plume, using the  
 18  $\Sigma$ PNs methods (confirmed also by other methods), but the low (or negative) R values suggest a  
 19 different origin for these plumes. Summarizing, we classified three flights (highlighted in grey in  
 20 Table 3) with evidence of significant BB plumes sampled, three with a small percentage of BB plumes  
 21 and 8 flights with a dominance of background air masses sampled. Le Breton et al. (2013) evaluated  
 22 the percentage of flights ascribable as BB plumes using the  $6\sigma$  method applied to their HCN  
 23 measurements and the R<sup>2</sup> between the CO and the HCN in the BB plumes for five flights. Our results,  
 24 with the percentage of flight identified as BB plume using their method, are in agreement with those  
 25 that they presented, with the exception of the B621 flight. In this case, the difference could be due to  
 26 the fact that we split the double flights into two datasets and also because for the B621b there are  
 27 some missing data for the HCN and only one big plume. Moreover, the R<sup>2</sup> between HCN and CO  
 28 range between 0.46 (B622) and 0.83 (B621) (Le Breton et al., 2013).  
 29 Figure 2 shows the scatter plot between the  $\Sigma$ PNs and the CO for the flights B621a, B622 and B623:  
 30 the red circles are the BB plume selected by the  $6\sigma$  of the  $\Sigma$ PNs technique and the green circles the  
 31 background part of each flight



1 **Figure 2.** Scatter plot between the  $\Sigma$ PNs and the CO for the B621a, B622 and B623 flights (from the  
2 top to the bottom, respectively). The red points indicate the data selected as BB plume using the 6 $\sigma$   
3 method to the  $\Sigma$ PNs measurements, the green points indicate the background air masses.



1 The  $\Sigma$ PNs show a very good correlation with the CO, in presence of BB plumes: the correlation  
2 coefficients R, in fact, vary between 0.804 and 0.953. The data of the B623 flight (Figure 2) show an  
3 interesting, well distinct double trends between the  $\Sigma$ PNs and the CO; the time series (Figure 1)  
4 shows that the CO and the CH<sub>3</sub>CN present two plumes (between  $8.2 \times 10^4$ -  $8.4 \times 10^4$  seconds A.M. and  
5 between  $8.6 \times 10^4$ - $8.8 \times 10^4$  seconds A.M.) at pressure (P) higher than ~750 hPa (corresponding to an  
6 altitude of ~2000 m a.s.l.): at these plumes do not correspond an increase of the  $\Sigma$ PNs nor of the  
7 Furfural. In order to explain the double trends in the  $\Sigma$ PNs vs CO scatter plot of the flight B623 (see  
8 figure 2), we analysed the all dataset of this flight as function of the pressure, finding that the two  
9 trends can be distinguished using a pressure threshold of 750 hPa (Figure 3), or equivalently an  
10 altitude threshold of ~2000 m a.s.l. (not shown).

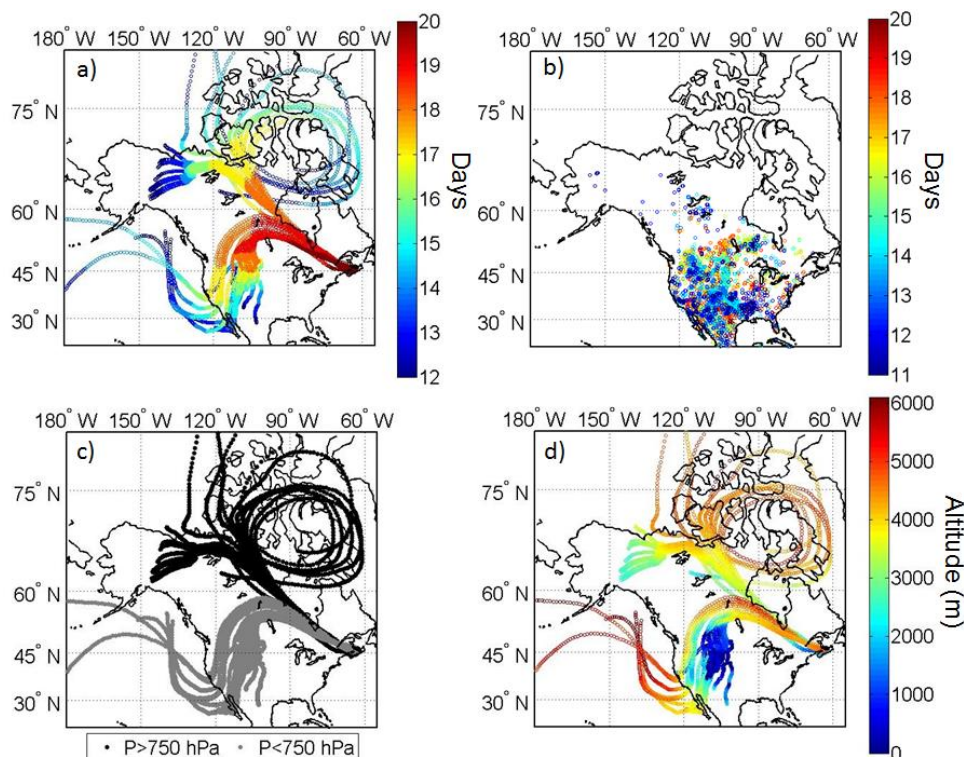


11  
12 **Figure 3.** Scatter plot between the  $\Sigma$ PNs and the CO as function of the pressure of the flight B623.

13  
14 The fact that the two distinct trends of the flight B623 are separable by the  $6\sigma$  method of the  $\Sigma$ PNs  
15 and by pressure, suggests that the air masses sampled at different altitude are originated by different  
16 sources, and the smaller correlation ( $R = 0.31$ ) between  $\Sigma$ PNs and CO for pressure above 750 hPa,  
17 supports the hypothesis that they are not impacted by BB emission. To prove this thesis, we evaluated  
18 the lagrangian back-trajectories (Hysplit model, Draxler et al., 1999) selecting the starting point at  
19 different altitudes along the flight trajectory and running the model up to 200 hours back. Panel c) in  
20 Figure 4 shows the black-trajectories of air masses sampled at pressure higher than 750 hPa (black  
21 points) or lower than 750 hPa (grey points): a different origin is clearly identifiable. In particular, air  
22 masses collected at lower altitudes ( $P > 750$  hPa) come from the northern region of the Canada and  
23 the altitude of provenience increases the further back the trajectory goes and decreases in the last  
24 three days of simulation (Figure 4d); on the contrary the air masses corresponding to  $P < 750$  hPa



1 originated in the South-West region of the Canada (e.g., Alberta, Saskatchewan,...) and in the North-  
2 West states of the U.S.A. (e.g., Montana, Idaho, Wyoming, Washington, Oregon,...). Figure 4a  
3 represents the position of the air masses along the back-trajectories during the days between the July  
4 12<sup>th</sup> and July 20<sup>th</sup> (corresponding respectively to -200 hours back and 0 hours back in the back-  
5 trajectories model setup). In the same way, Figure 4b shows the fire spots recorded by the FLAMBE  
6 (The Fire Locating And Monitoring of Burning Emissions, Reid et al., 2009) archives as function of  
7 the day in which the biomass burning occurred (between the July 11<sup>th</sup> and July 20<sup>th</sup>). The Figure 4  
8 reveals not only that air masses collected for  $P > 750$  hPa come from a different region of the North  
9 America respect to those collected for  $P < 750$  hPa, but also that the regions of interest for air masses  
10 at  $P > 750$  hPa are, most likely, not impacted by fire emissions, at least for the days in which the air  
11 masses passed over those areas. On the contrary, the plumes (identified as BB plumes) measured at  
12  $P < 750$  hPa (i.e. altitude higher than 2000 m a.s.l.) have originated from regions strongly influenced  
13 by biomass burning fires (see panel b of figure 4) in the central-west coast of the North America)  
14 in the days of July in which the air masses flew above those territories. The back-trajectories analysis,  
15 therefore, confirm the existence of two different layers of air masses sampled during the B623 flight  
16 distinguishable by the pressure (i.e. the altitude).



17

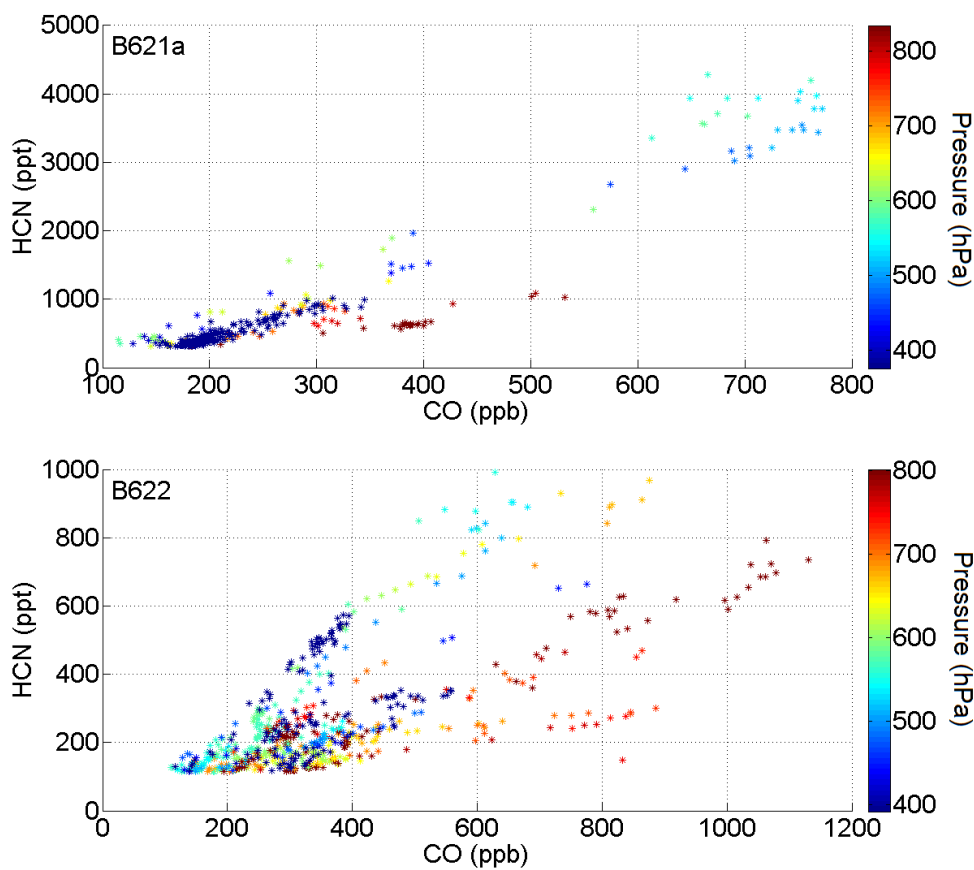


1 **Figure 4.** Panel a): temporal position (express as day from the 12<sup>th</sup> July to the 20<sup>th</sup> of July) along the  
2 200 hours back-trajectories. Panel b): spot of the biomass burning fires derived from the FLAMBE  
3 archive as function of the day in which they occurred (from 11<sup>th</sup> July to 20<sup>th</sup> July – we selected the  
4 dataset at the 13.00 UTC and the 23.00 UTC). Panel c): distinction of the back trajectories position  
5 selecting the starting point along the flight trajectories for  $P \geq 750$  hPa. Panel d): altitude along the  
6 back trajectories.

7  
8 Finally, we evaluated the qualitative age of the air masses sampled during the B623 flight: using the  
9 ratio between the NO<sub>x</sub> (sum of the TD-LIF NO<sub>2</sub> and the chemiluminescence NO measurements) and  
10 the total NO<sub>y</sub> (measured by the TD-LIF and the calculated as sum of NO<sub>x</sub> and its oxidation products),  
11 we observed that the air masses sampled at  $P < 750$  hPa are younger respect those sampled at higher  
12 pressure confirming that the air masses identifiable by the pressure are distinct not only for their  
13 sources (and provenience), but also for the age.

14 Considering what has been highlighted analysing the double trends in the CO vs  $\Sigma$ PNs plot of the  
15 B623, we examined in depth the correlation between the CO and the  $\Sigma$ PNs for all the flights and we  
16 found that also other flights show similar trends: in fact, B621a and the B622 show two different  
17 trends that can be distinguished using a pressure threshold of 700 hPa (figure not shown). Moreover,  
18 we did the same analysis also for the HCN: we found that for the B621a, B622 the scatter plot (plotting  
19 only the data selected as BB plume using the Le Breton et al. (2013) method) between the HCN and  
20 the CO shows different trends that can be distinct by the pressure (Figure 5, panel a and b related to  
21 the B621a and B622 flight, respectively). This analysis suggest that, even though the identification  
22 of a BB plume done using different chemical species threshold is largely and successfully employed  
23 (Le Breton et al., 2013; Lewis et al., 2013; Palmer et al., 2013; O’Shea et al. 2013), there are some  
24 episodes in which the introduction of other parameters (such as the pressure or the altitude, which are  
25 indicative of the vertical position of the air masses and, therefore, may be particularly significant for  
26 observations on-board aircrafts) gives interesting information and allow to discriminate better and  
27 with more details the plumes. The back-trajectories evaluation also gives an important indication of  
28 the origin of the air masses and completes the analysis.

29



1

2

3 **Figure 5.** Scatter plot between the HCN and the CO as function of the pressure for the flights B621a  
4 (at the top) and B622 (at the bottom).

5

#### 6 **4. Model results**

7 In order to refine the methods to discriminate the BB plumes and better understand the origin of the  
8 air masses analysed in the BORTAS campaign, an artificial neural network (ANN) model, recently  
9 developed for O<sub>3</sub> and PM studies (Biancofiore et al., 2015a; Biancofiore et al., 2015b), has been  
10 adapted and used with BORTAS dataset. The ANN is capable of simulating non-linear relationships  
11 (Lonbladd et al. 1992) and for this reason is ideal for investigating the relationship between  $\Sigma$ PNs  
12 (and HCN) and chemical and physical parameters. In this work, a recurrent architecture was used  
13 (Elman, 1990) that provides a multi-step memory. We simulated the concentrations of the  $\Sigma$ PNs for  
14 the B623 flight and of the  $\Sigma$ PNs and the HCN for the B622. During both these flights the scatter plots  
15 between the  $\Sigma$ PNs and the CO or the HCN and the CO show different trends that we distinguished  
16 by the pressure and that are indicative of air masses having different origins (coming from regions



1 interested by fires or not), as explained in Section 3. We carried out two different simulations: a) we  
2 used as input for the neural network only the O<sub>3</sub>, CO, NO and CH<sub>3</sub>CN (case A); b) we used as input  
3 the O<sub>3</sub>, CO, NO, CH<sub>3</sub>CN and the pressure (case B). In this way, we evaluated if and how the  
4 simulations of the  $\Sigma$ PNs and the HCN change by adding a physical parameter to the inputs, therefore  
5 taking into account the position of the air masses (that is the altitude of the aircraft during the flights).  
6 Figure 6 shows the results of the case A simulations for the flight B622: the scatter plot between the  
7 simulated HCN (panel a) and  $\Sigma$ PNs (panel b) and the measured CO as function of the pressure does  
8 not present distinct trends as evident in the measured data. Similar results have been found for the  
9 case A simulations (panel c in Figure 6) of the flight B623: the net separation of two trends in the  
10  $\Sigma$ PNs vs CO scatter plot of the measured data (Figure 2) is not reproduced by the model. On the  
11 contrary, adding the pressure to the inputs (case B) the simulations improve significantly for both the  
12 flights and both the species; Figure 7 shows the ANN simulations in the case B. It is evident that the  
13 different trends, identifiable by the pressure using the measured data (Figure 3 and Figure 5), are well  
14 reproduced and become evident despite what occurred in the case A (Figure 6). Moreover, it is clear  
15 also that the correlation coefficients between the  $\Sigma$ PNs measured and the  $\Sigma$ PNs simulated increase  
16 adding the pressure to the inputs (these results are highlighted in grey in Table 4): in fact, R improves  
17 from 0.94 (case A) to 0.95 (case B) for the B622 flight and, even more, from 0.77 (case A) to 0.94  
18 (case B) for the flight B623, in which the two trends between the  $\Sigma$ PNs and the CO is significantly  
19 more evident respect to the B622 flight. Similar results can be found for the HCN: the correlation  
20 coefficient R, in fact, increases from 0.86 (case A) to 0.92 (case B). In addition to the correlation  
21 coefficient R, we estimated the model performances using three more typical indices (Biancofiore et  
22 al., 2015): the fractional bias (FB), the normalized mean squared error (NMSE) and the factor of 2  
23 (FA2). The results are summarized in Table 4. The FB is calculated as the ratio between the difference  
24 of the mean observed and the mean modelled concentrations and their mean; it indicates the systemic  
25 errors that can entail a bias between the modelled and the measured data and can range between -2  
26 (overestimation) and +2 (underestimation): an ideal model has an FB index of 0. The NMSE is the  
27 result of the ratio between the mean of the squared difference between the observed and the modelled  
28 concentrations and the sum of their mean; it gives information about the total errors of the models  
29 and the best value is 0 (as the NMSE decreases approaching 0, the model performance increases).  
30 Finally, the FA2 is the percentage of the simulated data for which the ratio between the observed and  
31 the modelled concentrations is included between 0.5 and 2; the ideal model has an FA2 of 1 and the  
32 worst results occur if FA2 is equal to 0. The  $\Sigma$ PNs simulation for the flight B622 shows that R, NMSE  
33 and the FA2 improve adding the pressure to the inputs (case B); on the contrary, the FB results slightly  
34 worst indicating that the model tends to overestimate the concentrations. The HCN simulation for the



1 flight B622 has better results for all the indices with the exception, also in this case, of the FB which  
 2 is lightly greater in the case B than in the case A. Finally, the R, FB and FA2 of the  $\Sigma$ PNs modelled  
 3 for the flight B623 show a significant improvement in the case B respect the case A, but the NMSE  
 4 presents a worsening suggesting the possibility of an increase in the systemic or random errors.

5

6 **Table 4.** Indices to evaluate the Model performances. R is the correlation coefficient, FB is the  
 7 fractional bias, NMSE is the normalized mean squared error and FA2 the factor of 2. See the text for  
 8 a description of these indices

	Simulations	R	FB	NMSE	FA2
$\Sigma$ PNs (B622)	Case A	0.94	-0.017	0.124	0.755
	Case B	0.95	-0.023	0.099	0.763
HCN (B622)	Case A	0.86	0.009	0.228	0.946
	Case B	0.92	0.014	0.136	0.959
$\Sigma$ PNs (B623)	Case A	0.77	0.014	0.028	0.771
	Case B	0.94	-8.8e-4	0.079	0.867

9

10

11

12

13

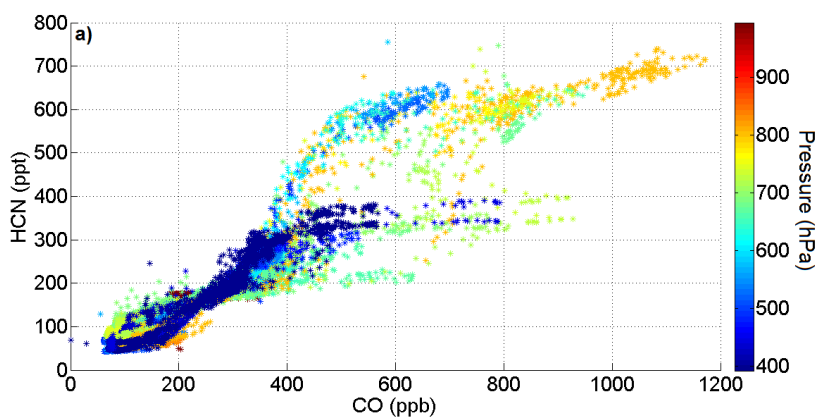
14

15

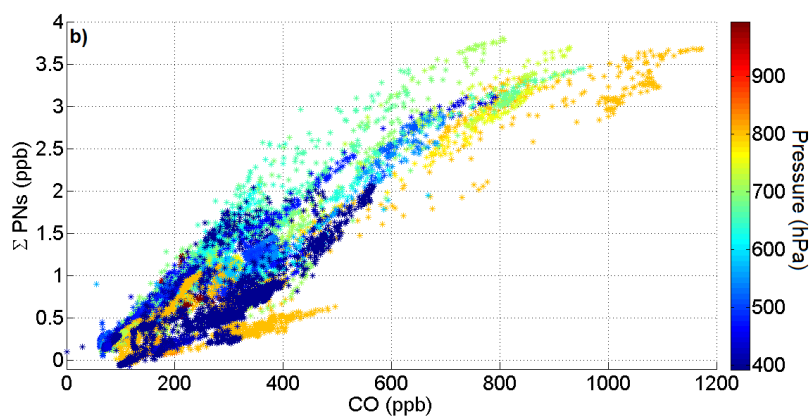
16



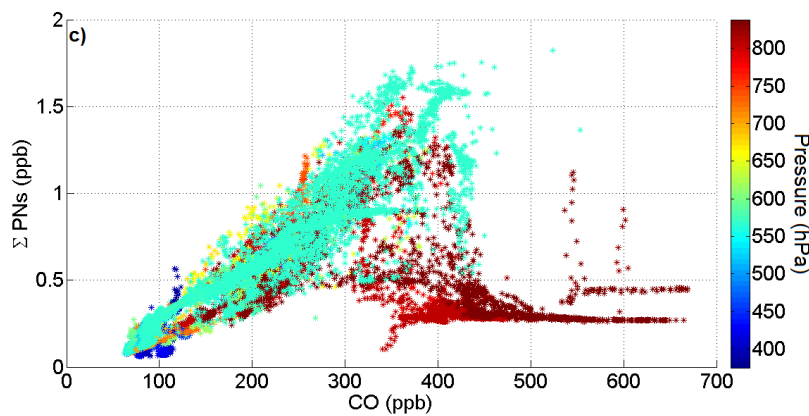
1



2



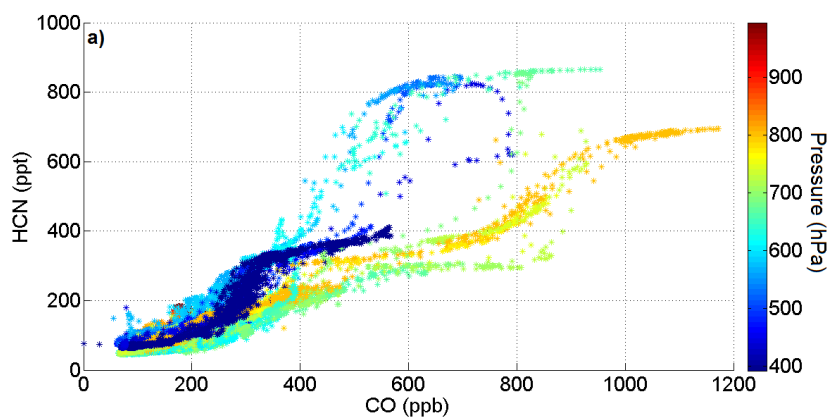
3



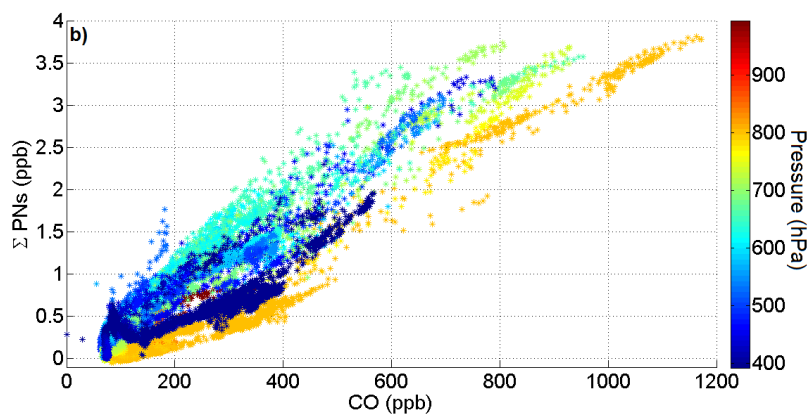
4 **Figure 6.** Simulations results for the case A (only O<sub>3</sub>, CO, NO and CH<sub>3</sub>CN as inputs): scatter plot  
5 between the simulated HCN (panel a)), the simulated ΣPNs (panel b)) and the CO for the B622 and  
6 between the simulated ΣPNs and CO for the B622 (panel a)) and the B623 (panel b)).



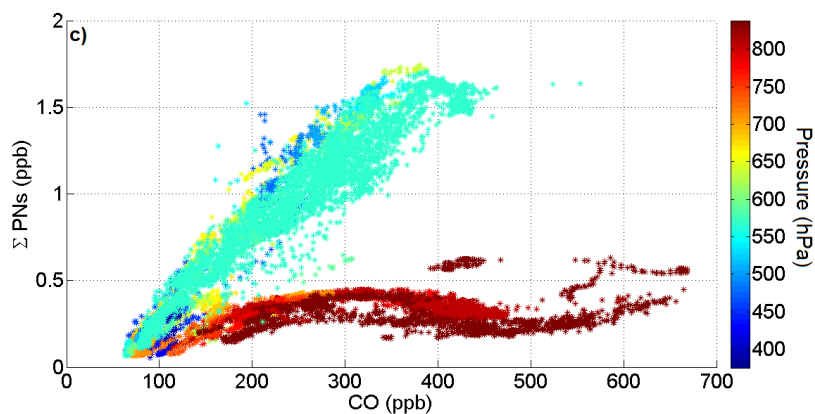
1



2



3



4 **Figure 7.** Simulations results for the case B ( $O_3$ , CO, NO,  $CH_3CN$  and pressure as inputs): scatter  
5 plot between the HCN (panel a)) simulated and the CO for the B622 and between  $\Sigma$ PNs and CO for  
6 the B623 (panel b)).



## 1 **Conclusions**

2 The measured  $\Sigma$ PNs during the BORTAS aircraft campaign show a good correlation (R varying  
3 between ~0.80 and ~0.95) with CO for different flights. We used  $\Sigma$ PNs as BB tracers applying two  
4 different methods to select a BB plumes: 1) we defined a threshold of  $6\sigma$  of  $\Sigma$ PNs concentration for  
5 each flights and all the data that are  $6\sigma$  times higher than the background level have been selected as  
6 BB plume; 2) evaluating the 99<sup>th</sup> percentile of the  $\Sigma$ PNs measurements done during the B625 flight  
7 (considered a background flight not affected by BB plumes). Moreover, we applied several methods  
8 present in the literature to our dataset to compare with the proposed  $\Sigma$ PNs methods and we calculated  
9 the percentage of flight classifiable as BB plume; we found that all the methods identified four flights  
10 with evident and significant percentage of BB plumes intercepted. Therefore for most of the flights  
11 the  $\Sigma$ PNs methods can be an alternative to identify BB. Moreover, we found that in some flights the  
12 scatter plot between the  $\Sigma$ PNs and the CO (or the HCN and the CO) shows different slopes  
13 identifiable by a pressure threshold, suggesting different regimes between these species that is  
14 different air masses. The dependency of these slopes by the pressure suggested that the air masses  
15 sampled could be spatially (vertically) different and that their origins could be different. Analysing  
16 the back-trajectories, as expected, we found that the air masses were not all originated by biomass  
17 burning and that those at lower pressure (i.e. higher altitude) reach Nova Scotia from the clean  
18 northern region of the Canada. In order to refine the method we adapted an ANN model simulating  
19 the  $\Sigma$ PNs and the HCN in two different ways: 1) using only the CO, NO and CH<sub>3</sub>CN as inputs; 2)  
20 adding also the pressure to the inputs. We found that the model results improve in the second case.  
21 In conclusion, we suggest that the  $\Sigma$ PNs can be used as BB tracer for the identification of BB plumes;  
22 moreover, as consequence of the  $\Sigma$ PNs vs CO analysis and of the model results, we suggest that the  
23 use of a meteorological parameter (such as pressure) could allow a better discrimination of the air  
24 masses origin and a more selective method for the selection of BB plumes.

25

## 26 **Acknowledgements**

27 The BORTAS project was supported by the Natural Environment Research Council (NERC) under grant  
28 number NE/F017391/1.

29

## 30 **References**

31

32 Alvarado, M. J., Logan, J. A., Mao, J., Apel E, Riemer, D., Blake, D., Cohen, R. C., Min, K.-E.,  
33 Perring, A. E., Browne, E.C., Wooldridge, P. J., Diskin, G. S., Sachse, G.W., Fuelberg, H.,  
34 Sessions, W. R., Harrigan, D. L., Huey, G., Liao, J., Case-Hanks, A., Jimenez, J. L., Cubison, M.



- 1 J., Vay, S. A., Weinheimer, A. J., Knapp, D. J., Montzka, D. D., Flocke, F. M., Pollack, I. B.,  
2 Wennberg, P. O., Kurten, A., Crounse, J., St. Clair, J. M., Wisthaler, A., Mikoviny, T., Yantosca,  
3 R. M., Carouge, C. C., and Le Sager, P.: Nitrogen oxides and PAN in plumes from boreal fires  
4 during ARCTAS-B and their impact on ozone: an integrated analysis of aircraft and satellite  
5 observations, *Atmos. Chem. Phys.*, 10, 9739–9760, 2010.
- 6 Andreae, M. O. and Merlet, P.: Emission of trace gases and aerosols from biomass burning, *Global*  
7 *Biogeochem. Cy.*, 15, 955–966, 2001.
- 8 Biancofiore, F., Verdecchia, M., Di Carlo, P., Tomassetti, B., Aruffo, E., Busilacchio, M., Bianco,  
9 S., Di Tommaso, S., Colangeli, C.: Analysis of surface ozone using a recurrent neural network,  
10 *Sci. Total. Environ.*, 514, 379–387, 2015a.
- 11 Biancofiore, F., Busilacchio, M., Verdecchia, M., Tomassetti, B., Aruffo, E., Bianco, S., Di  
12 Tommaso, S., Colangeli, C., and Di Carlo, P.: Forecasting PM10 and PM2.5 using a recursive  
13 neural network model, *Atmospheric Res.*, *under review*, 2015b.
- 14 Bertschi, I. T., Jaffe, D. A., Jaegle, L., Price, H. U., and Dennison, J. B.: PHOBEA/ITCT 2002  
15 airborne observations of trans-Pacific transport of ozone, CO, VOCs, and aerosols to the  
16 northeast Pacific: Impacts of Asian anthropogenic emissions and Siberian boreal fire emissions,  
17 *J. Geophys. Res.*, D23S12, doi:10.1029/2003JD004328, 2004.
- 18 Cofer III, W. R., Winstead, E. L., Stocks, B. J., Goldammer, J. G., and Cahoon, D. R.: Crown fire  
19 emissions of CO<sub>2</sub>, CO, H<sub>2</sub>, CH<sub>4</sub>, and TNMHC from a dense jack pine boreal forest fire,  
20 *Geophys. Res. Lett.*, 25, 3919–3922, 1998.
- 21 Crutzen, P. J., Andreae, M. O.: Biomass Burning in the Tropics: Impact on Atmospheric Chemistry  
22 and Biogeochemical Cycles, *Science*, Vol. 250 no. 4988 pp. 1669–1678, 1990.
- 23 Crutzen, P.J., Heidt, L.E., Krasnec, J.P., Pollock W.H., and Seiler, W.: Biomass burning as a source  
24 of atmospheric gases CO, H<sub>2</sub>, N<sub>2</sub>O, NO, CH<sub>3</sub>Cl and COS. *Nature*, 282, 253–256, 1979.
- 25 Dari-Salisburgo, C., Carlo, P. D., Giammaria, F., Kajii, Y., and D’Altorio, A.: Laser induced  
26 fluorescence instrument for NO<sub>2</sub> measurements: Observations at a central Italy background  
27 site, *Atmos. Environ.*, 43, 970–977, 2009.
- 28 Day, D. A., Wooldridge, P. J., Dillon, M. B., Thornton, J. A., and Cohen, R. C.: A thermal dissociation  
29 laser-induced fluorescence instrument for in-situ detection of NO<sub>2</sub>, peroxy nitrates, alkyl nitrates,  
30 and HNO<sub>3</sub>, *J. Geophys. Res.*, 107(D6), 4046, doi:10.1029/2001JD000779, 2002.



- 1 Di Carlo, P., Aruffo, E., Busilacchio, M., Giammaria, F., Dari-Salisburgo, C., Biancofiore, F.,  
2 Visconti, G., Lee, J., Moller, S., Reeves, C. E., Bauguitte, S., Forster, G., Jones, R. L., and  
3 Ouyang, B.: Aircraft based four-channel thermal dissociation laser induced fluorescence  
4 instrument for simultaneous measurements of NO<sub>2</sub>, total peroxy nitrate, total alkyl nitrate, and  
5 HNO<sub>3</sub>, Atmos. Meas. Tech., 6, 971–980, doi:10.5194/amt-6-971-2013, 2013.
- 6 Draxler, R. R.: HYSPLIT4 user's guide, Tech. Rep. NOAA Tech. Memo. ERL ARL-230, NOAA Air  
7 Resources Laboratory, Silver Spring, MD, 1999.
- 8 Dibb, J. E., Talbot, R. W., Scheuer, E. M., Seid, G., Avery, M. A., and Singh, H. B.: Aerosol chemical  
9 composition in Asian continental outflow during the TRACE-P campaign: Comparison with  
10 PEM-West B, J. Geophys. Res., 108(D21), 8815, doi:10.1029/2002JD003111, 2003.
- 11 Elman L.J.: Finding structure in time. Cognitive Science. 14, 179–211, 1990.
- 12 Gerbig, C., Schmitgen, S., Kley, D., Volz-Thomas, A., Dewey, K., and Haaks, D.: An improved fast-  
13 response vacuum-UVresonance fluorescence CO instrument, J. Geophys. Res., 104 (D1), 1699–  
14 1704, 1999.
- 15 Gillett, N., Weaver, A. J., Zwiers, F. W., and Flannigan, M. D.: Detecting the effect of climate change  
16 on Canadian forest fires, Geophys. Res. Lett., 31, L18211, doi:10.1029/2004GL020876, 2004.
- 17 Goode, J. G., Yokelson, R. J., Ward, D. E., Susott, R. A., Babbitt, R. E., Davies, M. A., and Hao, W.  
18 M.: Measurements of Excess O<sub>3</sub>, CO<sub>2</sub>, CO, CH<sub>4</sub>, C<sub>2</sub>H<sub>4</sub>, C<sub>2</sub>H<sub>2</sub>, HCN, NO, NH<sub>3</sub>, HCOOH,  
19 CH<sub>3</sub>COOH, HCHO and CH<sub>3</sub>OH in 1997 Alaskan Biomass Burning Plumes by Airborne Fourier  
20 Transform Infrared Spectroscopy (AFTIR), J. Geophys. Res., 105, 22147–22166, 2000.
- 21 Holzinger, R., Williams, J., Salisbury, G., Klupfel, T., de Reus, M., Traub, M., Crutzen, P. J., and  
22 Lelieveld, J.: Oxygenated compounds in aged biomass burning plumes over the Eastern  
23 Mediterranean: evidence for strong secondary production of methanol and acetone, Atmos.  
24 Chem. Phys., 5, 39–46, 2005.
- 25
- 26 Hopkins, J. R., Read, K. A., and Lewis, A. C.: Two column method for long-term monitoring of non-  
27 methane hydrocarbons (NMHCs) and oxygenated volatile organic compounds, J.  
28 Environ. Monitor., 5, 8–13, 2003.
- 29 Hornbrook, R. S., Blake, D. R., Diskin, G. S., Fried, A., Fuelberg, H. E., Meinardi, S., Mikoviny, T.,  
30 Richter, D., Sachse, G. W., Vay, S. A., Walega, J., Weibring, P., Weinheimer, A. J., Wiedinmyer,  
31 C., Wisthaler, A., Hills, A., Riemer, D. D., and Apel, E. C.: Observations of nonmethane organic



- 1 compounds during ARCTAS –Part 1: Biomass burning emissions and plume enhancements,  
2 Atmos. Chem. Phys., 11, 11103–11130, 2011.
- 3 Hudman, R.C., Jacob, D.J., Turquety, S., Leibensperger, E.M., Murray, L.T., Wu, S., Gilliland, A.,  
4 Avery, M., Bertram, T., Brune, W., Cohen, R., Dibb, J., Flocke, F., Fried, A., Holloway, J.,  
5 Neuman, J., Orville, R., Perring, A., Ren, X., Sachse, G., Singh, H., Swanson, A., and  
6 Wooldridge, P.: Surface and lightning sources of nitrogen oxides over the United States:  
7 Magnitudes, chemical evolution, and outflow, J. Geophys. Res., 112, D12S05,  
8 doi:10.1029/2006JD007912, 2007.
- 9 Jacob, D. J., Wofsy, S. C., Bakwin, P. S., Fan, S.-M., Harriss, R.C., Talbot, R.W., Bradshaw, J.,  
10 Sandholm, S., Singh, H. B., Gregory, G. L., Browell, E. V., Sachse, G. W., Blake, D. R., and  
11 Fitzjarrald, D. R.: Summertime photochemistry at high northern latitudes, J. Geophys. Res., 97,  
12 16421–16431, 1992.
- 13 Jaffe, D.A., and Wigder, N.L.: Ozone production from wildfires: A critical review. Atmospheric  
14 Environment 51, 1–10, doi:10.1016/j.atmosenv.2011.11.063, 2012.
- 15 Lavoué D., Liousse C., Cachier H., Stocks B.J., and Goldammer J.G.: Modeling of carbonaceous  
16 particles emitted by boreal and temperate wildfires at northern latitudes. J. Geophys. Res.:  
17 Atmos. 105(D22): 26871-26890, 2000.
- 18 Le Breton, M., Bacak, A., Muller, J. B. A., O'Shea, S. J., Xiao, P., Ashfold, M. N. R., Cooke, M. C.,  
19 Batt, R., Shallcross, D. E., Oram, D. E., Forster, G., Bauguitte, S. J.-B., Palmer, P. I.,  
20 Parrington, M., Lewis, A. C., Lee, J. D., and Percival, C. J.: Airborne hydrogen cyanide  
21 measurements using a chemical ionisation mass spectrometer for the plume identification of  
22 biomass burning forest fires, Atmos. Chem. Phys., 13, 9217-9232, doi:10.5194/acp-13-9217-  
23 2013, 2013.
- 24 Lee, J. D., Moller, D. J., Read, K. A., Lewis, A. C., Mendes, L., and Carpenter, L. J.: Year-round  
25 measurements of nitrogen oxides and ozone in the tropical North Atlantic marine boundary layer,  
26 J. Geophys. Res., 114, D21302, doi:10.1029/2009JD011878, 2009
- 27 Leung, F.-Y. T., Logan, J. A., Park, R., Hyer, E., Kasischke, E., Streets, D., and Yurganov, L.: Impacts  
28 of enhanced biomass burning in the boreal forests in 1998 on tropospheric chemistry and the  
29 sensitivity of model results to the injection height of emissions, J. Geophys. Res., 112, D10313,  
30 doi:10.1029/2006JD008132, 2007.
- 31 Lewis, A. C., Evans, M. J., Methven, J., Watson, N., Lee, J. D., Hopkins, J. R., Purvis, R. M., Arnold,  
32 S. R., McQuaid, J. B., Whalley, L. K., Pilling, M. J., Heard, D. E., Monks, P. S., Parker, A. E.,



- 1 Reeves, C. E., Oram, D. E., Mills, G., Bandy, B. J., Stewart, D., Coe, H., Williams, P., and  
2 Crosier, J.: Chemical composition observed over the mid-Atlantic and the detection of pollution  
3 signatures far from source regions, *J. Geophys. Res.*, 112, D10S39, doi:10.1029/2006JD007584,  
4 2007.
- 5 Lewis, A. C., Evans, M. J., Hopkins, J. R., Punjabi, S., Read, K. A., Purvis, R. M., Andrews, S. J.,  
6 Moller, S. J., Carpenter, L. J., Lee, J. D., Rickard, A. R., Palmer, P. I., and Parrington, M.: The  
7 influence of biomass burning on the global distribution of selected non-methane organic  
8 compounds, *Atmos. Chem. Phys.*, 13, 851–867, [www.atmos-chem-phys.net/13/851/2013/](http://www.atmos-chem-phys.net/13/851/2013/), 2013.
- 9 Lonbladd L., Peterson C., and Rönngvaldsson T.: Pattern recognition in high energy physics with  
10 artificial neural network – Jetnet 2.0., *Comput. Phys. Comm.* 70, 167–182, 1992.
- 11 Marlon, J. R., Bartlein, P. J., Carcaillet, C., Gavin, D. G., Harrison, S. P., Higuera, P. E., Joos,  
12 F., Power, M. J., and Prentice, I. C.: Climate and human influences on global biomass burning  
13 over the past two millennia, *Nature Geoscience*, 1, 69–702, 2008.
- 14 Mauzerall, D., Jacob, D. J., Fan, S.-M., Bradshaw, J., Gregory, G., Sachse, G., and Blake, D.: Origin  
15 of tropospheric ozone at remote high northern latitudes in summer, *J. Geophys. Res.*, 101, 4175–  
16 4188, 1996.
- 17 Murphy, J. G., Oram, D. E., and Reeves, C. E.: Measurements of volatile organic compounds over  
18 West Africa, *Atmos. Chem. Phys.*, 10, 5281–5294, doi: 10.5194/acp-10-5281-2010, 2010.
- 19 O’Shea, S. J., Allen, G., Gallagher, M. W., Bauguitte, S. J.-B., Illingworth, S. M., Le Breton, M.,  
20 Muller, J. B. A., Percival, C. J., Archibald, A. T., Oram, D. E., Parrington, M., Palmer, P. I., and  
21 Lewis, A. C., Airborne observations of trace gases over boreal Canada during BORTAS:  
22 campaign climatology, air masses analysis and enhancement ratios, *Atmos. Chem. Phys.*, 13,  
23 12451–12467, 2013.
- 24 Palmer, P. I., Parrington, M., Lee, J. D., Lewis, A. C., Rickard, A. R., Bernath, P. F., Duck, T. J.,  
25 Waugh, D. L., Tarasick, D. W., Andrews, S., Aruffo, E., Bailey, L. J., Barrett, E., Bauguitte, S.  
26 J.-B., Curry, K. R., Di Carlo, P., Chisholm, L., Dan, L., Forster, G., Franklin, J. E., Gibson, M.  
27 D., Griffin, D., Helmig, D., Hopkins, J. R., Hopper, J. T., Jenkin, M. E., Kindred, D., Kliever,  
28 J., Le Breton, M., Matthiesen, S., Maurice, M., Moller, S., Moore, D. P., Oram, D. E., O’Shea, S.  
29 J., Owen, R. C., Pagnello, C. M. L. S., Pawson, S., Percival, C. J., Pierce, J. R., Punjabi, S., Purvis,  
30 R. M., Remedios, J. J., Rotermund, K. M., Sakamoto, K. M., da Silva, A. M., Strawbridge, K. B.,  
31 Strong, K., Taylor, J., Trigwell, R., Tereszchuk, K. A., Walker, K. A., Weaver, D., Whaley, C.,  
32 and Young, J. C.: Quantifying the impact of Boreal forest fires on Tropospheric oxidants over



- 1 the Atlantic using Aircraft and Satellites (BORTAS) experiment: design, execution and science  
2 overview, *Atmos. Chem. Phys.*, 13, 6239–6261, doi:10.5194/acp-13-6239-2013, 2013.
- 3 Parrington, M., Palmer, P. I., Henze, D. K., Tarasick, D. W., Hyer, E. J., Owen, R. C., Helmig, D.,  
4 Clerbaux, C., Bowman, K. W., Deeter, M. N., Barratt, E. M., Coheur, P.-F., Hurtmans, D., Jiang,  
5 Z., George, M., and Worden, J. R.: The influence of boreal biomass burning emissions on the  
6 distribution of tropospheric ozone over North America and the North Atlantic during  
7 2010, *Atmos. Chem. Phys.*, 12, 2077–2098, doi:10.5194/acp-12-2077-2012, 2012.
- 8 Purvis, R. M., Lewis, A. C., Hopkins, J. R., Andrews, S., and Minaean, J.: Functionalized aromatic  
9 compounds within middle troposphere boreal biomass burning plumes, in preparation, 2013.
- 10 Real, E., Law, K. S., Weinzierl, B., Fiebig, M., Petzold, A., Wild, O., Methven, J., Arnold, S., Stohl,  
11 A., Huntrieser, H., Roiger, A., Schlager, H., Stewart, D., Avery, M., Sachse, G., Browell, E.,  
12 Ferrare, R., and Blake, D.: Processes influencing ozone levels in Alaskan forest fire plumes  
13 during long-range transport over the North Atlantic, *J. Geophys. Res.*, 112,  
14 D10S41, doi:10.1029/2006JD007576, 2007.
- 15 Reid, J. S., Hyer, E. J., Prins, E. M., Westphal, D. L., Zhang, J., Wang, J., Christopher, S. A., Curtis,  
16 C. A., Schmidt, C. C., Eleuterio, D. P., Richardson, K. A., and Hoffman, J. P.: Global monitoring  
17 and forecasting of biomass burning smoke: Description of and lessons from the Fire Locating and  
18 Modeling of Burning Emissions (FLAMBE) program, *IEEE J. Sel. Top. Appl.*, 2, 144–162, 2009.
- 19 Reidmiller, D. R., Jaffe, D. A., Fischer, E. V., and Finley, B.: Nitrogen oxides in the boundary layer  
20 and free troposphere at the Mt. Bachelor Observatory, *Atmos. Chem. Phys.*, 10, 6043–  
21 6062, doi:10.5194/acp-10-6043-2010, 2010.
- 22 Rinsland, C. P., Dufour, G., Boone, C. D., Bernath, P. F., Chiou, L., Coheur, P.-F., Turquety, S., and  
23 Clerbaux, C.: Satellite boreal measurements over Alaska and Canada during June–July 2004:  
24 Simultaneous measurements of upper tropospheric CO, C<sub>2</sub>H<sub>6</sub>, HCN, CH<sub>3</sub>Cl, CH<sub>4</sub>, C<sub>2</sub>H<sub>2</sub>,  
25 CH<sub>3</sub>OH, HCOOH, OCS, and SF<sub>6</sub> mixing ratios, *Global Biogeochemical Cycles*, Vol. 21,  
26 GB3008, doi:10.1029/2006GB002795, 2007.
- 27 Tereszchuk, K. A., Gonzalez Abad, G., Clerbaux, C., Hurtmans, D., Coheur, P.-F., and Bernath, P.  
28 F.: ACE-FTS measurements of trace species in the characterization of biomass burning plumes,  
29 *Atmos. Chem. Phys.*, 11, 12169–12179, 2011.
- 30 Vay, S. A., Choi, Y., Vadrevu, K. P., Blake, D. R., Tyler, S. C., Wisthaler, A., Hecobian, A., Kondo,  
31 Y., G. S. Diskin, G. S., Sachse, G. W., Woo, J.-H., Weinheimer, A. J., Burkhardt, J. F., Stohl, A.,  
32 and Wennberg, P. O.: Patterns of CO<sub>2</sub> and radiocarbon across high northern latitudes during



- 1 International Polar Year 2008 , J. Geophys. Res., 116, D14301, doi:10.1029/2011JD015643,  
2 2011.
- 3 Val Martin, M., Honrath, R., Owen, R. C., Pfister, G., Fialho, P., and Barata, F.: Significant  
4 enhancements of nitrogen oxides, ozone and aerosol black carbon in the North Atlantic lower  
5 free troposphere resulting from North American boreal wildfires, J. Geophys. Res., 111, D23S60,  
6 doi:10.1029/2006JD007530, 2006.
- 7 Wilson, K. L. and Birks, J. W.: Mechanism and Elimination of a Water Vapor Interference in the  
8 Measurement of Ozone by UV Absorbance, Environmental Science and Technology 40, 6361-  
9 6367,2006.
- 10 Wofsy, S.C., Sachse, G.W., Gregory, G.L., Blake, D.R., Bradshaw, J.D., Sandholm, S.T., Singh,  
11 H.B., Barrick, J.A., Harriss, R.C., Talbot, R.W., Shipham, M.A., Browell, E.V., Jacob, D.J. and  
12 Logan, J.A.:Atmospheric chemistry in the Arctic and subarctic: Influence of natural fires,  
13 industrial emissions, and stratospheric inputs. J. Geophys. Res., 97: doi: 10.1029/92JD00622.  
14 issn: 0148-0227, 1992.
- 15 Wotawa, G., and Trainer, M.:The influence of Canadian forest fires on pollutant concentrations in  
16 the United States. Science 288(5464):324-328, 2000.
- 17